EasyChair Preprint

№ 15102

Constitutive Modeling of Fibrous Tissues with Non-Symmetric Fiber Dispersion: Application to Extension Behavior of Leather

Tonghuan Qu and Akihiro Matsuda

September 27, 2024

Constitutive modeling of fibrous tissues with non-symmetric fiber dispersion: Application to extension behavior of leather

Tonghuan QU[1, a] and Akihiro MATSUDA[2, b *]

[1]Graduate School of Systems and Information Engineering, University of Tsukuba,

1-1-1 Tennodai, Tsukuba City, Ibaraki 305-0006, Japan

[2]Institute of Systems and Information Engineering, University of Tsukuba,

1-1-1 Tennodai, Tsukuba City, Ibaraki 305-8573, Japan

[a] s2330204@u.tsukuba.ac.jp [b] a_matsuda@kz.tsukuba.ac.jp

Keywords: Anisotropy, Constitutive modeling, Computational mechanics, Finite element method, Leather material

Abstract. Leather is a fiber-reinforced material with a more concentrated fiber distribution in three dimensions perpendicular to the tangential plane than in-plane. The asymmetric dispersion of fibers can have a significant effect on the mechanical properties of natural leather. The transverse isotropic constitutive model is unable to accurately describe the anisotropy of natural leather. Accordingly, we have devised a novel anisotropic theoretical framework that incorporates asymmetric fiber dispersion, with the objective of accurately characterizing the mechanical behavior of anisotropy with asymmetric fiber distribution. Our approach entails the incorporation of the Yeoh model into the theoretical framework, as well as the introduction of a specific anisotropy term within the strain energy function, with the objective of describing the nonlinear properties. By fitting the theoretical results of the model to tensile test data of natural leather specimens, the structural and material parameters were determined. We provided specific stress tensors to enable finite element analysis. Our finite element analysis investigates the effect of asymmetric fiber dispersion on the mechanical response under uniaxial and biaxial stretching. By simulating the tensile behavior of natural leather specimens under different tensile angles, we observe a non-homogeneous stress distribution and non-homogeneous deformation due to fiber families under fixed stretching. This theoretical framework based on a continuum model provides a theoretical reference for describing the mechanical properties of leather materials with asymmetric fiber dispersion.

Introduction

The use of natural leather in the production of sports equipment is pervasive, largely due to the material's elasticity and waterproof properties. The strength of the leather material is significantly augmented by the existence of a fiber layer comprising two fiber families. The dispersion of fibers within the fiber layer gives the leather material complex anisotropic characteristics.

To describe such complex anisotropic properties, the intrinsic model [1] with transversely isotropic fiber dispersion may not be able to accurately describe the structural features of natural leather with asymmetric fiber dispersion. Instead, a constitutive model describing the asymmetric fiber dispersion in-plane and out-of-plane was proposed in [2], which is able to approximate the anisotropic characteristics of natural leather with different fiber dispersions in-plane and out-of-plane. Therefore, in this paper, a theoretical framework toward the anisotropy of natural leather is developed based on the constitutive model of asymmetric fiber dispersion. By introducing different specific forms of isotropic and anisotropic terms into the strain energy function, the form of the stress tensor is determined and the structural. The stress distribution and three-dimensional deformation of natural leather specimens are simulated by finite element implementation.

Anisotropic Mechanical Framework

Theoretical framework of non-symmetric fiber dispersion

Here we use the generalized structure tensor $\boldsymbol{H}$ of in-plane and out-of-plane separation proposed by [2] by importing the bivariate von Mises distribution to describe the non-symmetric fiber dispersion of natural leather, and the generalized structure tensor $\boldsymbol{H}$ is given by

$$\boldsymbol{H}=\sqrt{\frac{b}{2\pi^3}}\int_{\Phi=0}^{2\pi}\int_{\Theta=-\pi/2}^{\pi/2}\frac{\exp\left[a\cos 2\Phi+b(\cos 2\Theta-1)\right]}{I_0(a)\cdot\operatorname{erf}\left(\sqrt{2b}\right)}\boldsymbol{N}\otimes\boldsymbol{N}\cos\Theta\,\mathrm{d}\Phi\,\mathrm{d}\Theta \tag{1}$$

where Φ/Θ is the in-plane/out-of-plane Euler angle, a/b is the in-plane/out-of-plane concentration parameter and $\boldsymbol{N}$ is the unit vector representing any fiber direction. The related functions are given by

$$I_m(x)=\frac{1}{\pi}\int_0^{\pi}\cos m\varsigma\exp(x\cos\varsigma)\,\mathrm{d}\varsigma,\ \text{and}\quad \operatorname{erf}(x)=\frac{2}{\sqrt{\pi}}\int_0^{x}\exp\left(-\varsigma^2\right)\mathrm{d}\varsigma \tag{2}$$

respectively. The in-plane/out-of-plane dispersion parameter κ_{ip}/κ_{op}, which indicates the degree of in-plane/out-of-plane concentration fiber dispersion, is defined as

$$\kappa_{ip}=\kappa_{11}=\frac{1}{2}+\frac{I_1(a)}{2I_0(a)}\cos 2\alpha,\ \text{and}\quad \kappa_{op}=\frac{1}{2}-\frac{1}{8b}+\frac{1}{4}\sqrt{\frac{2}{\pi b}}\frac{\exp(-2b)}{\operatorname{erf}\left(\sqrt{2b}\right)} \tag{3}$$

where α is the angle between the two fiber families about the symmetry axis $\mathbf{e}_1$. The probability density functions over a unit sphere for different values of $\kappa_{op}(b)$ are represented as shown in Fig. 1. The form of $\boldsymbol{H}$ with respect to the mean direction $\boldsymbol{M}_i$, i=4, 6 of the i th fiber family is rewritten as

$$\boldsymbol{H}_i=A\boldsymbol{I}+B\boldsymbol{M}_i\otimes\boldsymbol{M}_i+(1-3A-B)\boldsymbol{M}_n\otimes\boldsymbol{M}_n,\quad i=4,6 \tag{4}$$

where A, B are the coefficients and $\boldsymbol{M}_\mathrm{n}$ is a unit vector in the out-of-plane, as shown in Fig. 2(a).

Continuum mechanical framework

The anisotropic mechanics framework is introduced. The deformation gradient $\boldsymbol{F}=\partial\boldsymbol{x}/\partial\boldsymbol{X}$ is defined as a spatial point $\boldsymbol{x}$ of the reference configuration Ω_0 deforms into the material point $\boldsymbol{X}$ of the current configuration Ω, and right Cauchy-Green tensor is defined as $\boldsymbol{C}=\boldsymbol{F}^{\mathrm{T}}\boldsymbol{F}$. According the approch proposed by [3], a multiplicative decomposition of $\boldsymbol{F}$ was performed.Thus, the modified deformation gradient and modified right Cauchy-Green tensor are defined as $\overline{\boldsymbol{F}}=J^{-1/3}\boldsymbol{F}$ and $\boldsymbol{C}=\overline{\boldsymbol{F}}^{T}\overline{\boldsymbol{F}}$, respectively, where $J=\det\boldsymbol{F}$ is the local volume ratio. The Green-Lagrange strain-like quantity $\overline{E}_i, i=4,6$, which represents the weighted fiber strain of mean direction $\boldsymbol{M}_i$, i=4, 6 is given by

$$\overline{E}_i=\boldsymbol{H}_i:\left(\overline{\boldsymbol{C}}-\boldsymbol{I}\right)=A\bar{I}_1+B\bar{I}_i+(1-3A-B)\bar{I}_n-1,\quad i=4,6 \tag{5}$$

where $\boldsymbol{I}$ denotes the identity tensor. $\bar{I}_i, i=4,6$ and $\bar{I}_n$ as the modified invariants are defined as

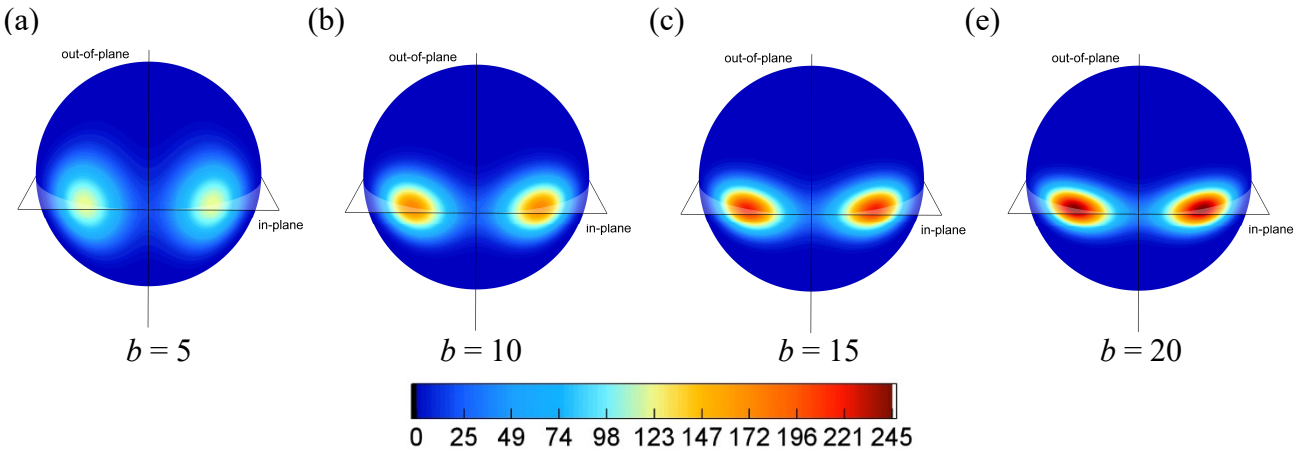

Fig. 1The probability densities of fiber families over a unit sphere for different values of out-of-plane concentration parameter: (a) b = 5, (b) b = 10, (c) b = 15 and (e) b = 20.

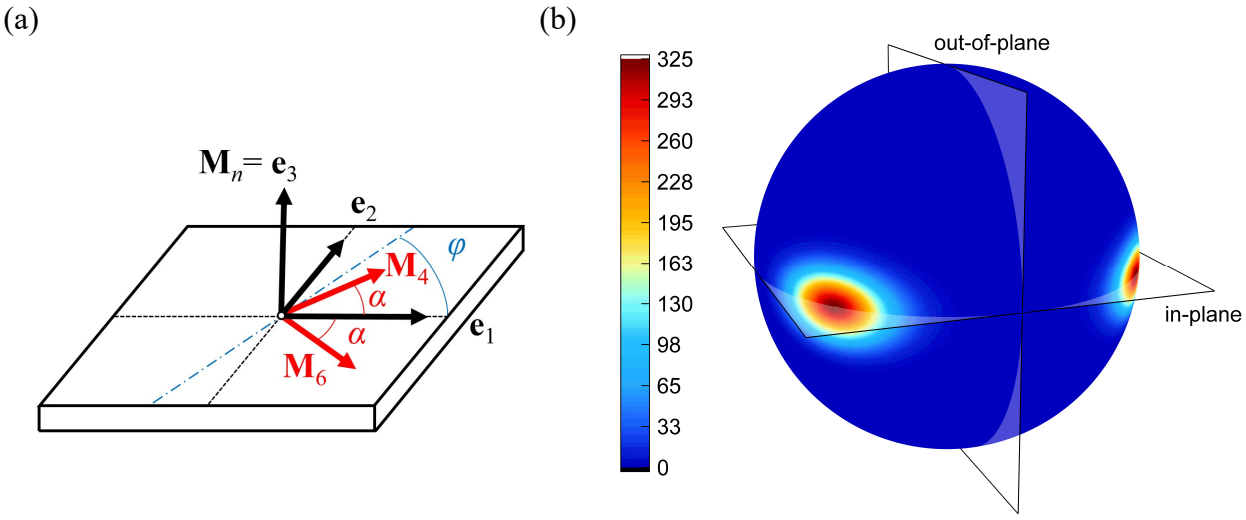

Fig. 2(a) Schematic diagram of natural leather with two fiber families $\boldsymbol{M}_4$ and $\boldsymbol{M}_6$. (b) The probability densities of two fiber families of natural leather specimens over a unit sphere.

$$\bar{I}_i = \bar{\boldsymbol{C}} : (\boldsymbol{M}_i \otimes \boldsymbol{M}_i), \quad i = 4, 6 \quad \text{, and } \bar{I}_n = \bar{\boldsymbol{C}} : (\boldsymbol{M}_n \otimes \boldsymbol{M}_n) \tag{6}$$

respectively. A decoupled form of the strain energy function Ψ was adopted, which can be decoupled.

$$\Psi(\boldsymbol{C}, \boldsymbol{H}) = \Psi^{\mathrm{o}}(J) + \bar{\Psi}_{iso}(\bar{\boldsymbol{C}}) + \sum_{i=4,6} \bar{\Psi}_{ani}(\bar{\boldsymbol{C}}, \boldsymbol{H}_i) \tag{7}$$

where $\bar{\Psi}_{\mathrm{iso}}$ and $\bar{\Psi}_{\mathrm{ani}}$ are the isotropic part and anisotropic part of the volumetric preserving term of Ψ. Thus, the corresponding decoupled form of second Piola–Kirchhoff stress tensor $\boldsymbol{S}$ is given by

$$\boldsymbol{S} = 2\frac{\partial \Psi}{\partial \boldsymbol{C}} = \bar{\boldsymbol{S}} + pJ\boldsymbol{C}^{-1}, \tag{8}$$

where the deviatoric part of second Piola–Kirchhoff stress tensor is calculated as

$$\begin{aligned} \bar{\boldsymbol{S}} &= 2\frac{\partial \bar{\Psi}}{\partial \boldsymbol{C}} = 2\left(\sum_{n=1,4,6} \frac{\partial \bar{\Psi}}{\partial \bar{I}_i}\frac{\partial \bar{I}_i}{\partial \boldsymbol{C}} + \frac{\partial \bar{\Psi}}{\partial \bar{I}_n}\frac{\partial \bar{I}_n}{\partial \boldsymbol{C}} \right) \\ &= 2J^{-\frac{2}{3}}\left[\frac{\partial \bar{\Psi}}{\partial \bar{I}_1}\left(\boldsymbol{I} - \frac{1}{3} I_1 \boldsymbol{C}^{-1} \right) + \sum_{i=4,6} \frac{\partial \bar{\Psi}}{\partial \bar{I}_i}\left(\boldsymbol{M}_i \otimes \boldsymbol{M}_i - \frac{1}{3} I_i \boldsymbol{C}^{-1} \right) + \frac{\partial \bar{\Psi}}{\partial \bar{I}_n}\left(\boldsymbol{M}_n \otimes \boldsymbol{M}_n - \frac{1}{3} I_n \boldsymbol{C}^{-1} \right) \right] \end{aligned} \tag{9}$$

And p denotes the hydrostatic pressure with $p = \mathrm{d}\Psi^{\mathrm{o}}(J)/\mathrm{d}J$.

Application to extension behavior of natural leather specimens

This section focuses on the tensile behavior of natural leather. A schematic diagram of natural leather is illustrated in Fig. 2(a), where φ represents the in-plane uniaxial stretch angle. According to the uniaxial tensile data of natural leather from our previous study [4], the structural parameters were determined and summarized in Table 1. The probability densities of the two fiber families of natural leather represented on the unit sphere are shown in Fig. 2(b). It can be seen that the out-of-plane fiber dispersion of natural leather specimens is characterized by a high degree of concentration.

A specific form of $\bar{\Psi}_{\mathrm{iso}}$ in Eq. (7), which was modeled after the Yeoh model, is defined as

$$\bar{\Psi}_{iso}(\boldsymbol{C}) = C_1(\bar{I}_1 - 3) + \frac{C_2}{2}(\bar{I}_1 - 3)^2 + \frac{C_3}{3}(\bar{I}_1 - 3)^3 \tag{10}$$

where C_i, i=1, 2, 3 are the material parameters associated with isotropy. The form of $\bar{\Psi}_{\mathrm{ani}}$, as follows:

$$\bar{\Psi}_{ani}(\boldsymbol{C}, \bar{\boldsymbol{H}}_i) = \frac{K_1}{2}\bar{E}_i^2 + \frac{K_2}{3}\bar{E}_i^3 + \frac{K_3}{4}\bar{E}_i^4, \quad i = 4, 6 \tag{11}$$

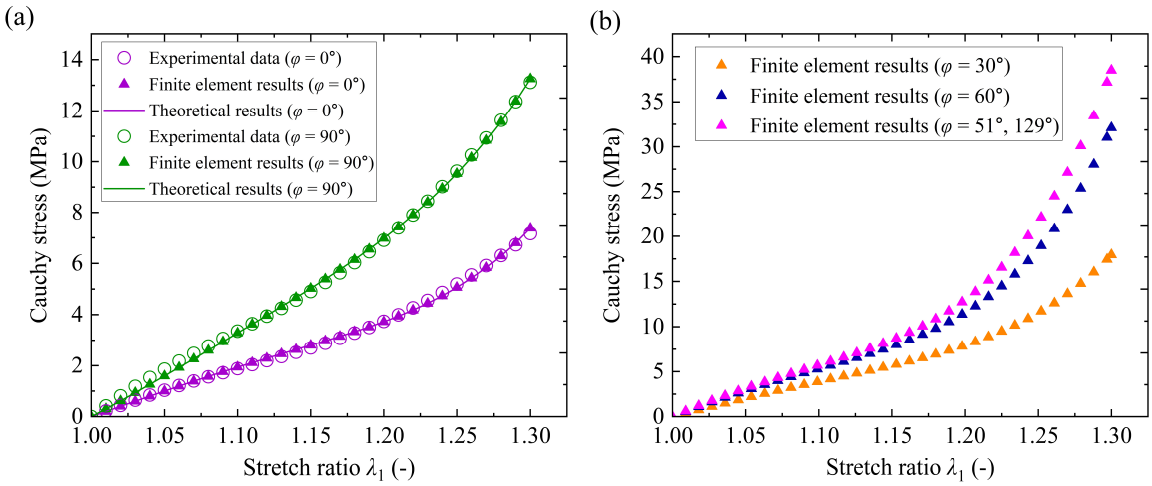

Fig. 3(a) Plot of Cauchy stress versus stretch λ_1 for φ = 0° and 90°, and corresponding experimental data and FE results. (b) Plot of FE results versus stretch λ_1 for φ = 30°, 60°, 51° and 129°.

where K_i, i=1, 2, 3 are the material parameters associated with anisotropy.

In this research, natural leather is considered to be a purely incompressible material (J = 1). By substituting the above specified energy function Ψ into Eq. 9, the specific form of the second Piola-Kirchhoff stress tensor for natural leather is obtained. It is calculated as follows:

$$\begin{aligned}\boldsymbol{S} &= \bar{\boldsymbol{S}} + p\boldsymbol{C}^{-1} = 2\left[C_1 + C_2(\bar{I}_1 - 3) + C_3(\bar{I}_1 - 3)^2\right]\left(\boldsymbol{I} - \frac{1}{3}I_1\boldsymbol{C}^{-1}\right) \\ &= 2\sum_{i=4,6}\left(K_1\bar{E}_i + K_2\bar{E}_i^{\,2} + K_3\bar{E}_i^{\,3}\right)\left[A\left(\boldsymbol{I} - \frac{1}{3}I_1\boldsymbol{C}^{-1}\right) + B\left(\boldsymbol{M}_i \otimes \boldsymbol{M}_i - \frac{1}{3}I_i\boldsymbol{C}^{-1}\right) + (1 - 3A - B)\left(\boldsymbol{M}_n \otimes \boldsymbol{M}_n - \frac{1}{3}I_n\boldsymbol{C}^{-1}\right)\right] + p\boldsymbol{C}^{-1}\end{aligned} \tag{12}$$

and the corresponding Cauchy stress is defined as $\boldsymbol{T} = \boldsymbol{FSF}^{\mathrm{T}}$. The theoretical results were fitted to the tensile results in [4] by the least squares method and the determined material parameters are also summarized in Table 1. And the corresponding coefficient of determination R^2 on φ = 0°and 90° are

Table 1 Determined structural and material parameters.

Structural parameters			Material parameters (MPa)			
out-of-plane	b		isotropy	C_1	C_2	C_3
	22.48			3.2556	-10.552	4.0886
in-plane	a	α	anisotropy	K_1	K_2	K_3
	7.75	51°		14.414	-41.722	67.880

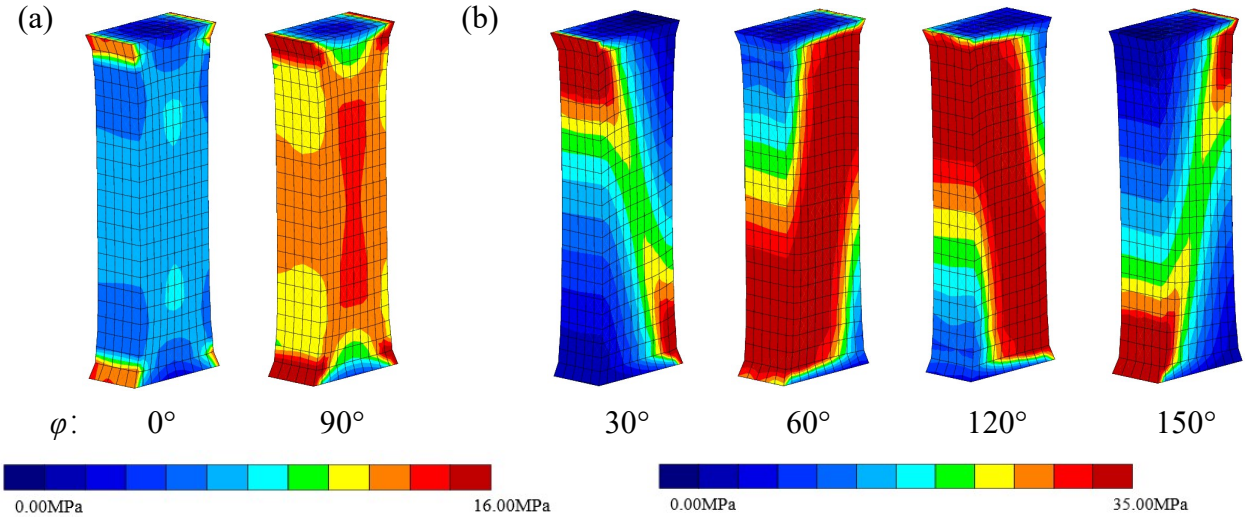

Fig. 4 Equivalent stress distributions of natural leather specimens stretched to λ = 1.3 for (a) φ = 0° and 90°, (b) φ = 30°, 60°, 120° and 150°.

99.83% and 99.87%, respectively, indicating a good fit to the experimental results.

The above anisotropic theoretical framework was imported into a finite element (FE) program, and FE simulations were performed for the same conditions. The experimental, theoretical, and FE results for $\varphi = 0°$ and 90° are represented in Fig. 3(a). It is observed that the FE results are in exact alignment with the theoretical results. Further uniaxial extension was simulated for $\varphi = 30°$, 60°, 51° and 129°, and the corresponding FE results are presented in Fig. 3(b). It can be seen that as the extension direction approaches the main direction of the fiber family, the stiffness of the natural leather increases. The greatest strength is observed when the stretching direction lies in the main direction of the fiber family (i.e., when $\varphi = 51°$ and 129°). The three-dimensional equivalent stress distributions at $\varphi = 0°$ and 90° are illustrated in Fig. 4(a). It can be observed that the stress distributions are symmetric about the symmetry axis of the two fiber families of natural specimen. The three-dimensional equivalent stress distributions at $\varphi = 30°$, 60°, 120° and 150° are represented in Fig. 4(b), all of which exhibit asymmetric in-plane equivalent stress distributions and three-dimensional deformation, exhibiting high equivalent stresses as φ approaches the main direction of the fiber family.

Effect of out-of-plane fiber dispersion of natural leather specimens

The effect of out-of-plane fiber dispersion of natural leather specimens is evaluated in this section. FE simulations of equibiaxial stretch of natural leather specimens along $\varphi = 30°$ were conducted. The relevant parameters listed in Table 1 were applied, with the exception of the out-of-plane dispersion parameter κ_{op}. Three cases with different values of κ_{op} are detailed in Table 2.

Table 2 Three cases of out-of-plane fiber dispersion of the natural leather specimens.

Case	Out-of-plane fiber dispersion	Out-of-plane dispersion parameter κ_{op}
I	Isotropy	$\kappa_{op} = 1/3$
II	Less concentration	$\kappa_{op} = 0.417$
III	High concentration	$\kappa_{op} = 0.499$

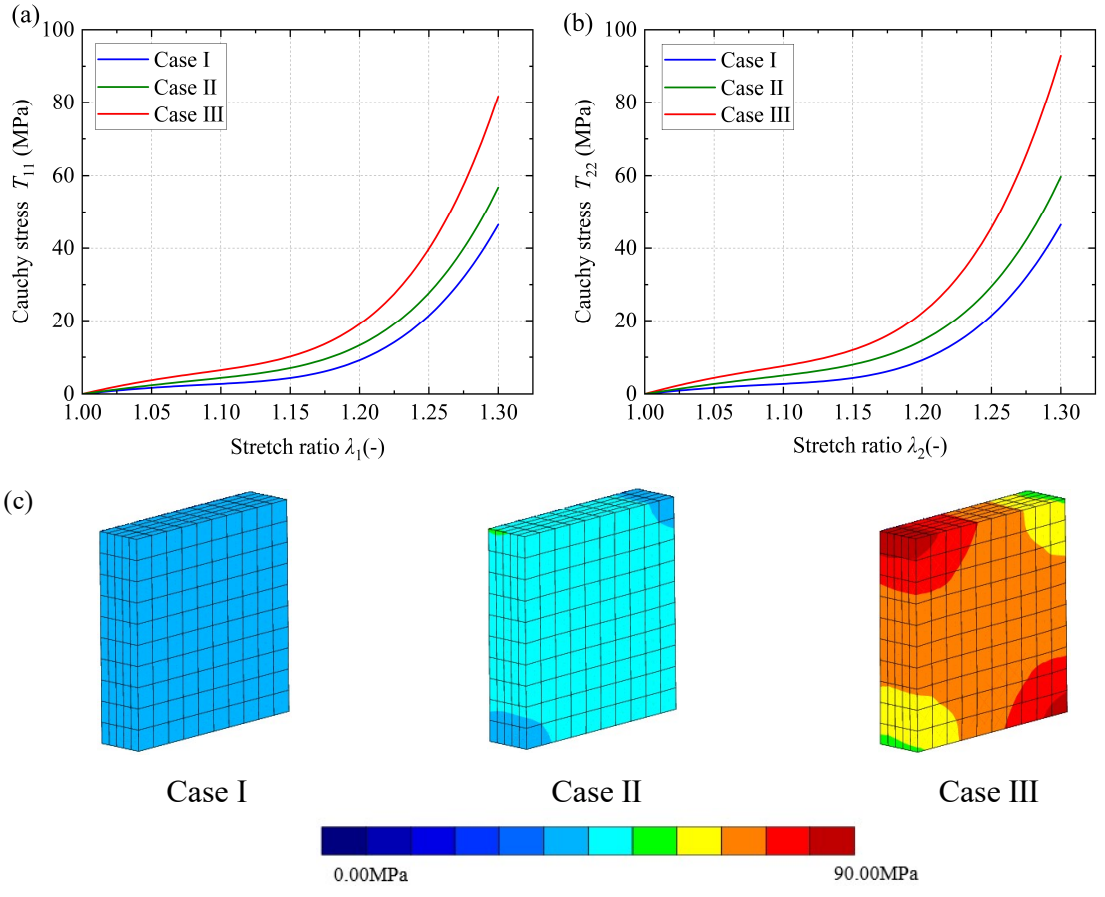

Fig. 5Plot of FE results versus stretch (a) λ_1 and (b) λ_2 for Cases I, II and III. (c) Equivalent stress distributions of natural leather specimens stretched equibiaxially to $\lambda = 1.3$ for Cases I, II and III.

The FE results for Cauchy stresses in the $\mathbf{e}_1$ and $\mathbf{e}_2$ directions for Cases I, II and III are presented in Fig. 5(a) and (b), respectively. The equivalent stress distributions of natural leather specimens stretched equibiaxially to a stretch ratio $\lambda = 1.3$ for different Cases are shown in Fig. 5(c). It can be seen that the mechanical responses in the two orthogonal directions in Case I are consistent and the equivalent stress distributions are equivalent, indicating isotropy. This is due to the uniform distribution of the out-of-plane fiber dispersion in any direction. In Case II, where the out-of-plane fiber dispersion is less concentrated, the stress in the $\mathbf{e}_2$ direction in proximity to the main direction of the fiber family is observed to be larger in comparison to another tensile direction, reflecting the anisotropic characteristics. Furthermore, the FE simulation of Case II indicates that the equivalent stresses are no longer uniformly distributed. In Case III, when the out-of-plane fiber dispersion is highly concentrated, the stresses in the two tensile directions are significantly enhanced. Moreover, the stresses in the $\mathbf{e}_2$ direction, which is near the main direction of the fiber family, are much higher than those in another tensile direction. As illustrated by the FE simulation of Case III, the equivalent stresses exhibit a significant inhomogeneous distribution. The results of the FE analysis of Cases I, II and III indicate that the effect of out-of-plane fiber dispersion on the anisotropic properties of natural leather is highly significant.

Conclusion

This research develops a theoretical framework for the anisotropy of natural leather by employing a constitutive model for asymmetric fiber distribution. The anisotropic structural parameters and material parameters were determined based on the tensile data of natural leather specimens, respectively. The tensile behavior of the natural leather specimens was implemented using a FE method, and the anisotropic properties of the specimens were evaluated by comparing the simulation results of three-dimensional deformation under uniaxial tensile at different angles. Furthermore, the effect of out-of-plane fiber dispersion on the tensile behavior of natural leather is investigated through the simulation of stress distribution in biaxial tensile testing of natural leather specimens with varying out-of-plane fiber dispersion. This provides a theoretical reference point for the analysis of three-dimensional deformation in sports equipment manufactured from natural leather material.

Acknowledgments

This research was supported in part by a grant 2024 (I) 9 from the Advanced Research Initiative for Human High Performance (ARIHHP), University of Tsukuba.

References

[1] T. C. Gasser, R. W. Ogden and G. A. Holzapfel, Hyperelastic modelling of arterial layers with distributed collagen fibre orientations, Journal of the Royal Society Interface, 3.6 (2006) 15-35.

[2] G. A. Holzapfel, J. A. Niestrawska, R. W. Ogden, A. J. Reinisch and A. J. Schriefl, Modelling non-symmetric collagen fibre dispersion in arterial walls, Journal of the Royal Society Interface, 12.106 (2015) 20150188.

[3] P. Flory, Thermodynamic relations for high elastic materials, Transactions of the Faraday Society, 57 (1961) 829-838.

[4] H. Nakahara, and A. Matsuda, Finite element computation with anisotropic hyperelastic model considering distributed fibers for artificial and natural leather used in sports, Mechanical Engineering Journal, 7.4 (2020) 20-00072.